Published in "Inorganic Chemistry 54(17): 8197–8206, 2015"
which should be cited to refer to this work.

Construction of Polynuclear Lanthanide (Ln= Dy^{III}, Tb^{III} and Nd^{III}) Cage Complexes using Pyridine-Pyrazole based ligands: Versatile Molecular Topologies and SMM behavior

Sukhen Bala,[a] Mousumi Sen Bishwas [b], Bhaskar Pramanik[c], Sumit Khanra, [c] Katharina M. Fromm[d] , Pankaj Poddar[b] and Raju Mondal[a]*

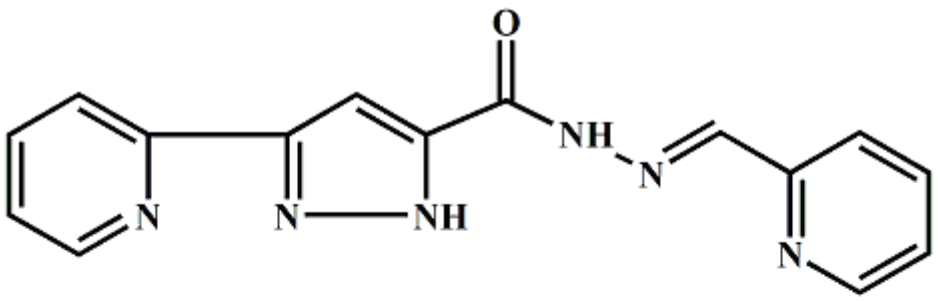

3-(pyridin-2-yl)-*N*'-((pyridin-2-yl)methylene)-1*H*-pyrazole-5-carbohydrazide(H_2L_1)

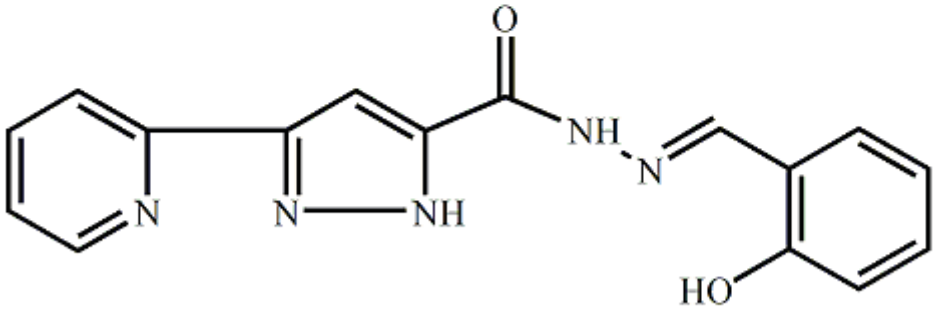

***N*'-(2-hydroxybenzylidene)-3-(pyridin-2-yl)-1*H*-pyrazole-5-carbohydrazide(H_3L_2)**

Figure S1: Schematic diagram of ligands.

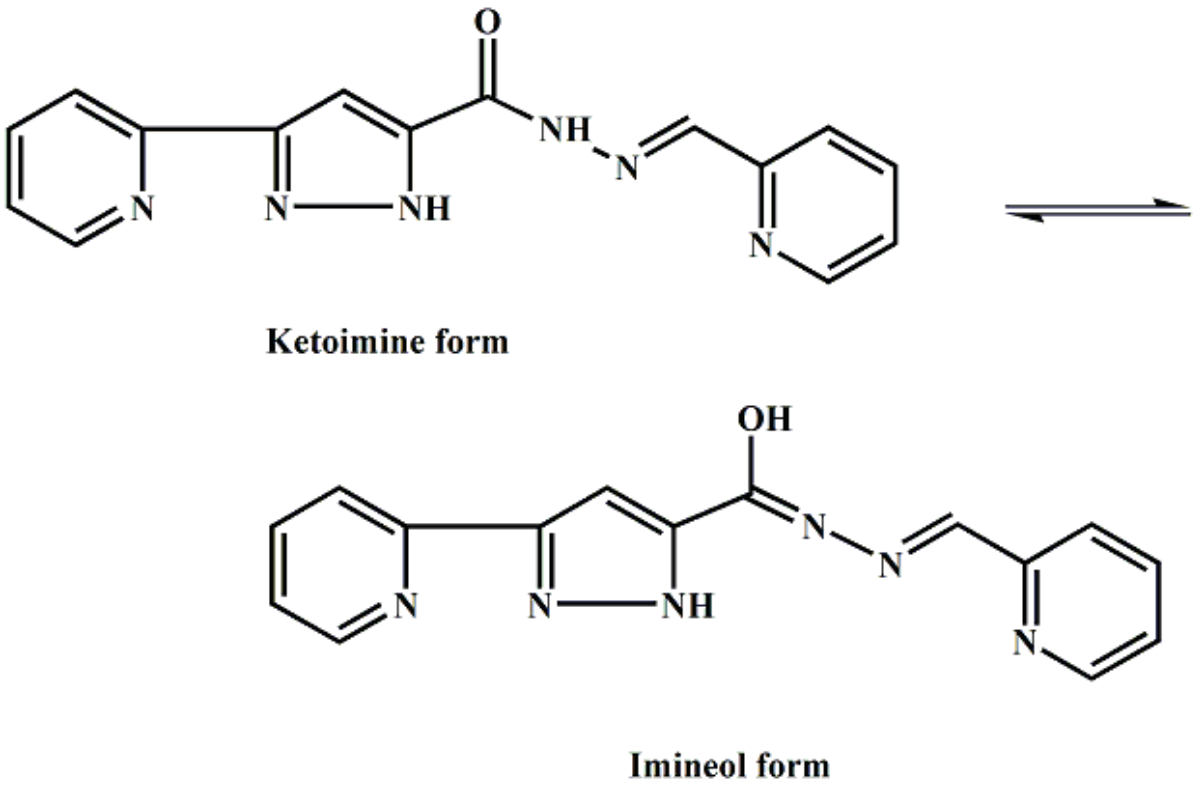

Figure S2: Keto–enol tautomerism of H_2L_1.

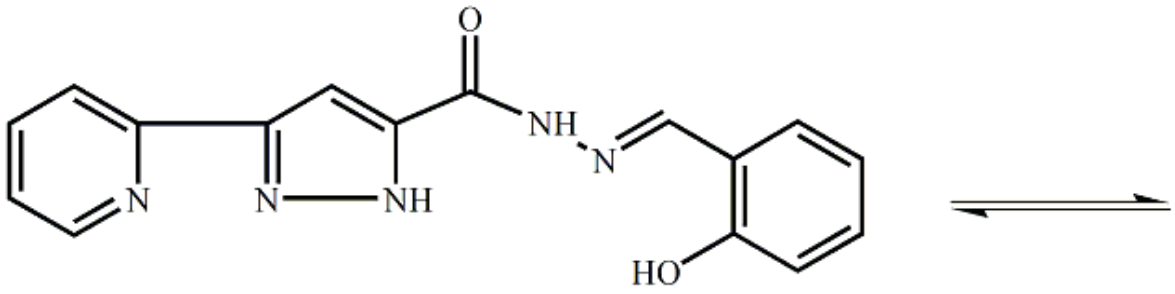

Ketoimine form

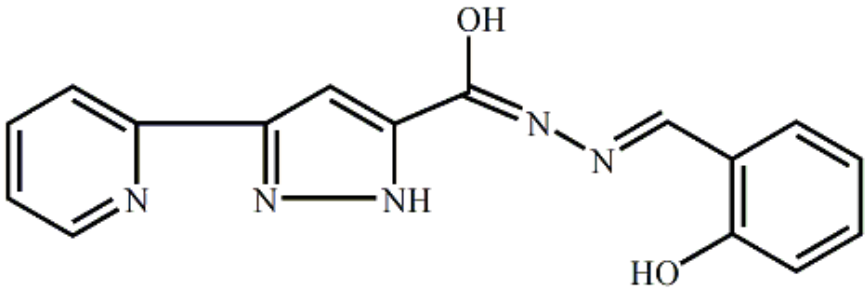

Imineol form

Figure S3: Keto–enol tautomerism of H_3L_2.

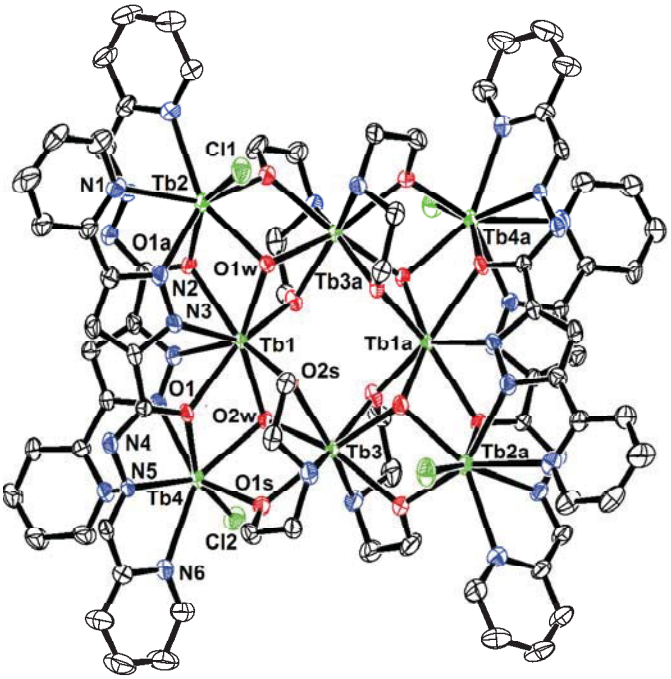

Figure S4. Perspective view of **2** with thermal ellipsoids at the 50% probability level. Hydrogen atoms are omitted for clarity.

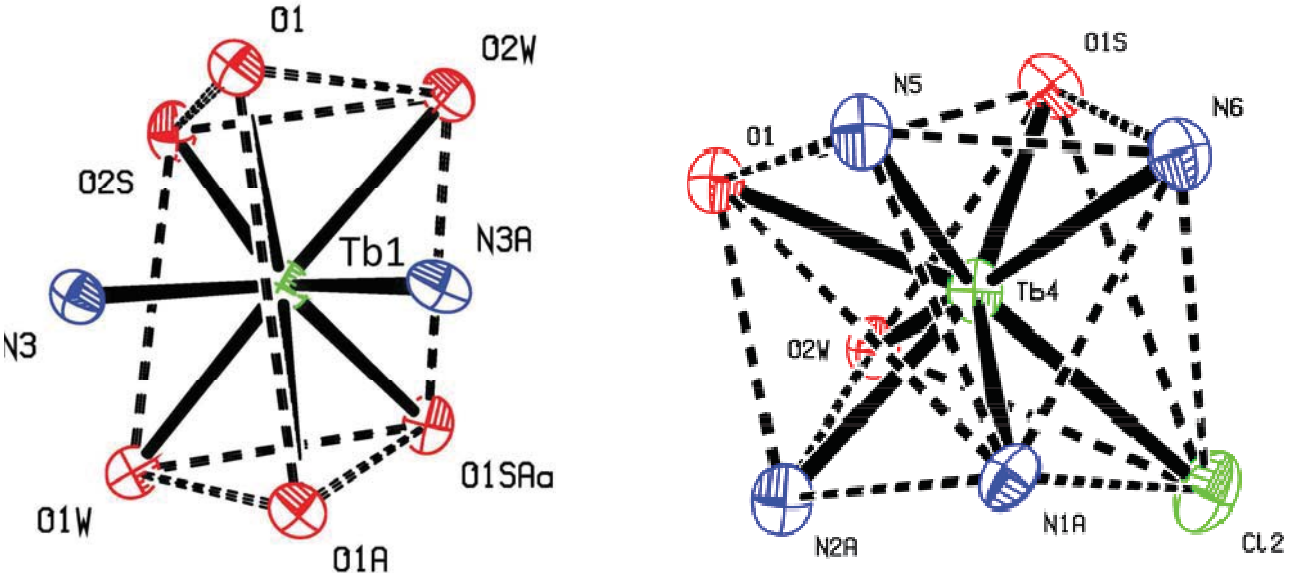

Figure S5. Representations of bicapped trigonal prism and distorted square antiprismatic geometry around Tb in **2**.

Luminescence Study:

Dy^{III} complexes 1 and 3 show very similar characteristic luminescence properties[S1]. Upon excitation at λ_{ex}= 265 nm, a strong luminescence is attributed to complexes 1 and 3. Both 1 and 3 exhibit typical blue emission peak at ~ 480 nm and another yellow emission peak at ~ 570 nm, characteristic for Dy^{III}.[S1] The blue emission is assigned to a $^4F_{9/2} \rightarrow {}^6H_{15/2}$ transition whereas the yellow emission is assigned to a $^4F_{9/2} \rightarrow {}^6H_{13/2}$ transition as shown in Figure S6. The spectra of **1** and **3** shown in Figures S6 clearly indicate that the intensity of the blue emission is much higher than that of the yellow emission. Furthermore, the complexes display additional peaks at ~ 482 and ~ 493 nm.

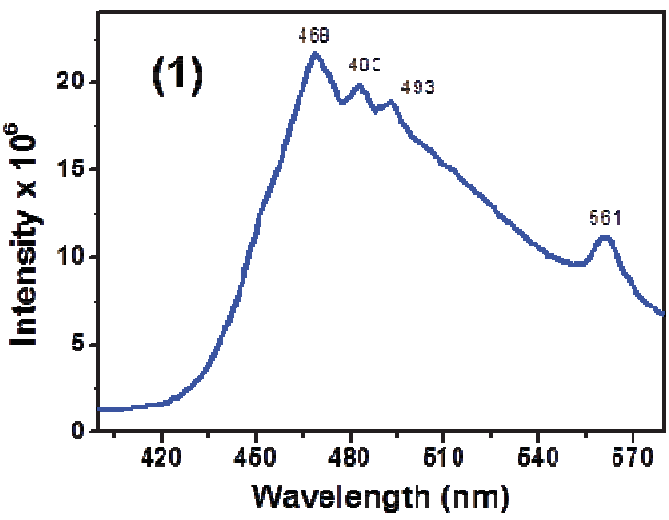

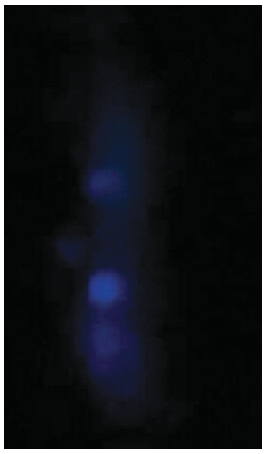

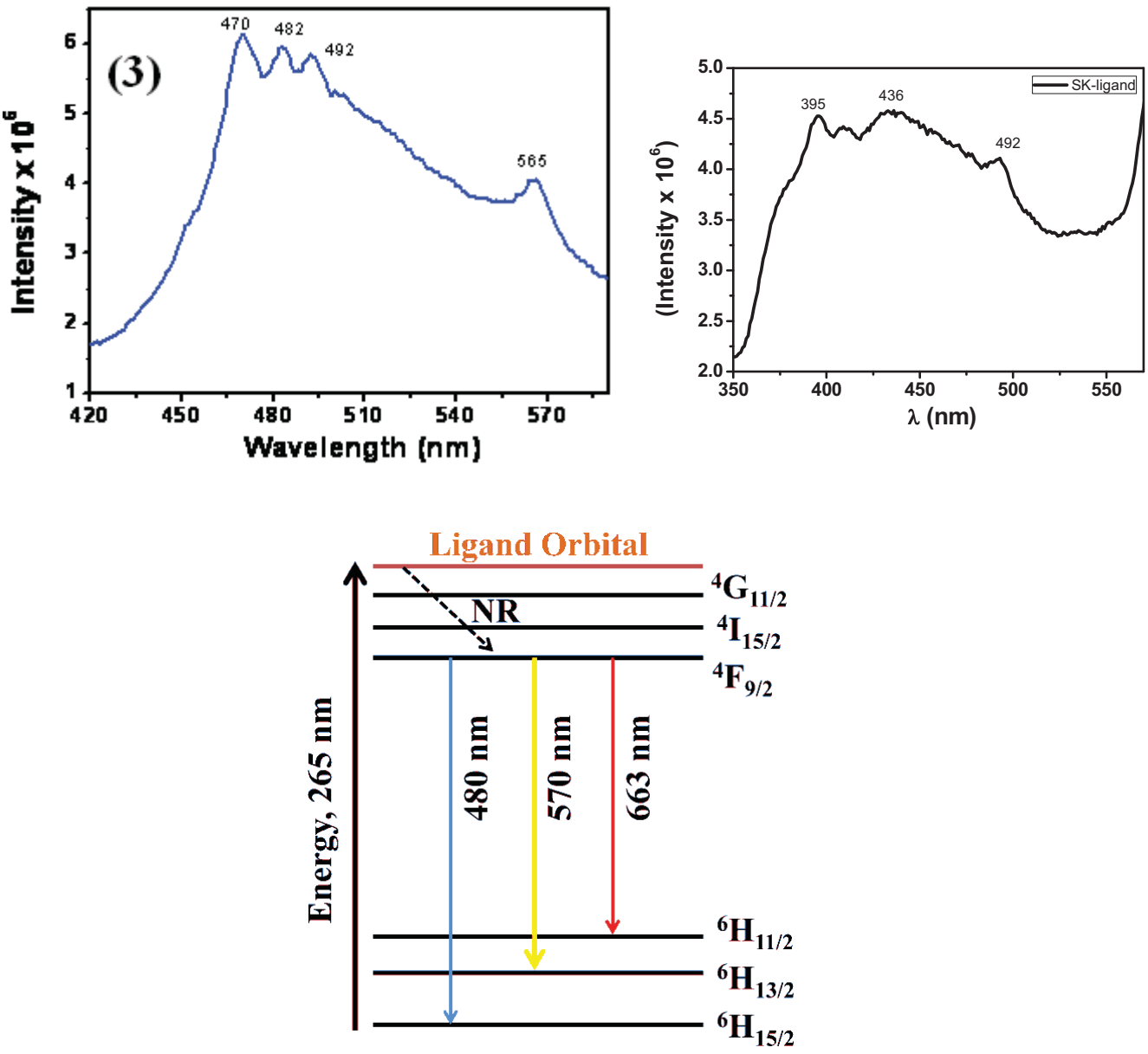

Figure S6. Solid state emission spectra of **1**, **3** and ligand at 298 K, excited at 265 nm and energy level diagrams of Dy^{III} showing possible transitions.

Magnetic data points below 50 K:

The χ_mT-T for all the three compounds **1**, **2**, and **3** were measured again below 50 K with more precision. Figure **S7**, **S8**, **S9** respectively shows the χ_mT-T plot for samples **1**, **2**, and **3** respectively. It was observed that the very small kink or anomaly that was seen ~ 27 K for compound **1** and **3** in early measurement was not visible when magnetization data were re-measured with more data points below 50 K.

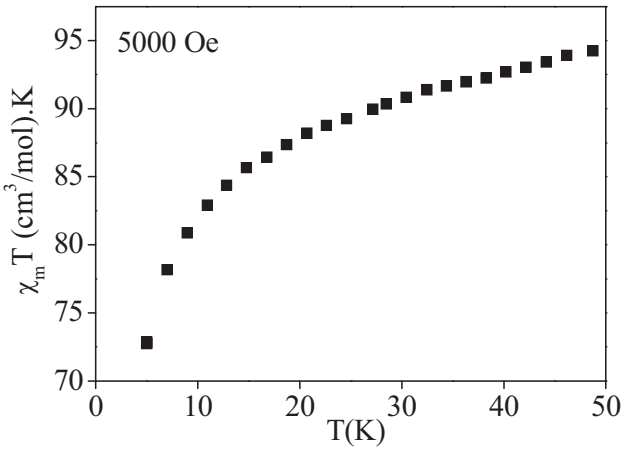

Figure S7. The χ_mT- T plot for the complex 1 under an applied field of 5000 Oe from 5 -50 K.

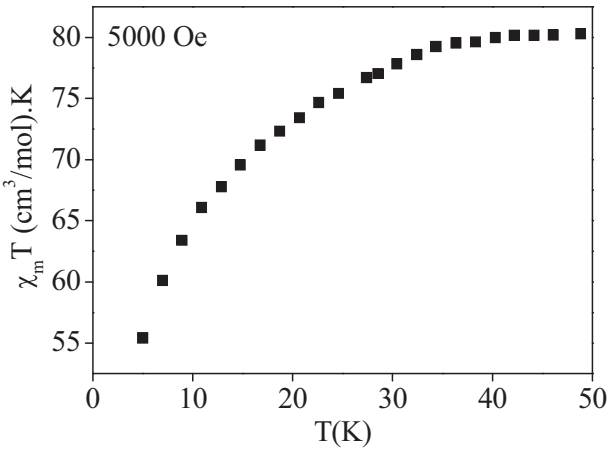

Figure S8. The χ_mT- T plot for the complex 2 under an applied field of 5000 Oe from 5 -50 K.

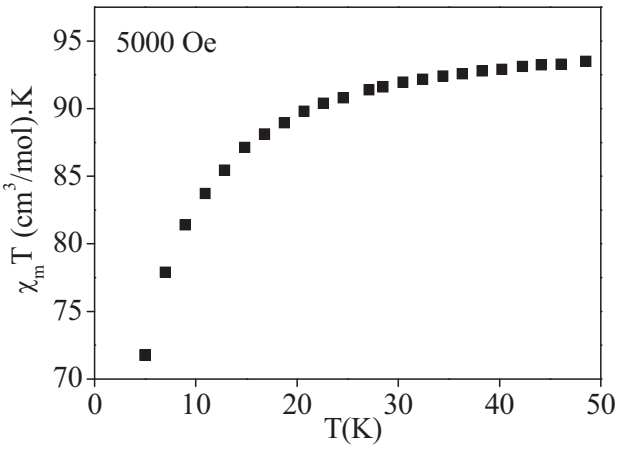

Figure S9. The χ_mT- T plot for the complex **3** under an applied field of 5000 Oe from 5 -50 K.

Frequency-dependent in-phase and out-of phase components of ac susceptibility of compound 1, 2 and 3:

The frequency dependence of compound **1**, **2**, and **3** from frequency 10 Hz to 1000 Hz are measured keeping temperature constant from 2 K to 20 K at an interval of 2 K. **Figures S10-S12,** show frequency dependence of in phase and out of phase component of susceptibility under zero dc field and 0.5 T dc field for compound **1-3**.

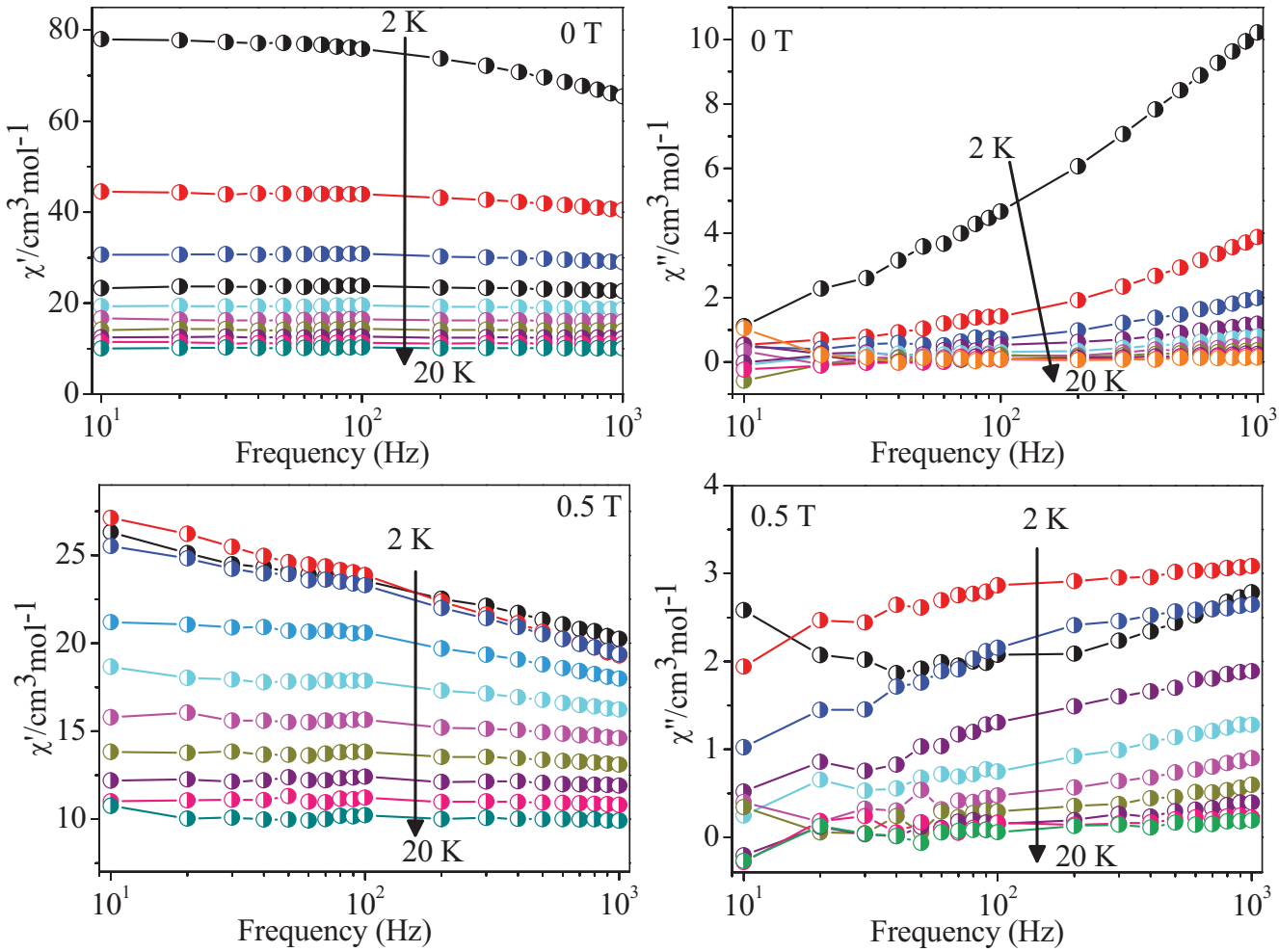

Figure S10: Frequency-dependent in-phase and out-of phase components of ac susceptibility of compound **1** under zero dc field (top) and 0.5 T field (bottom).

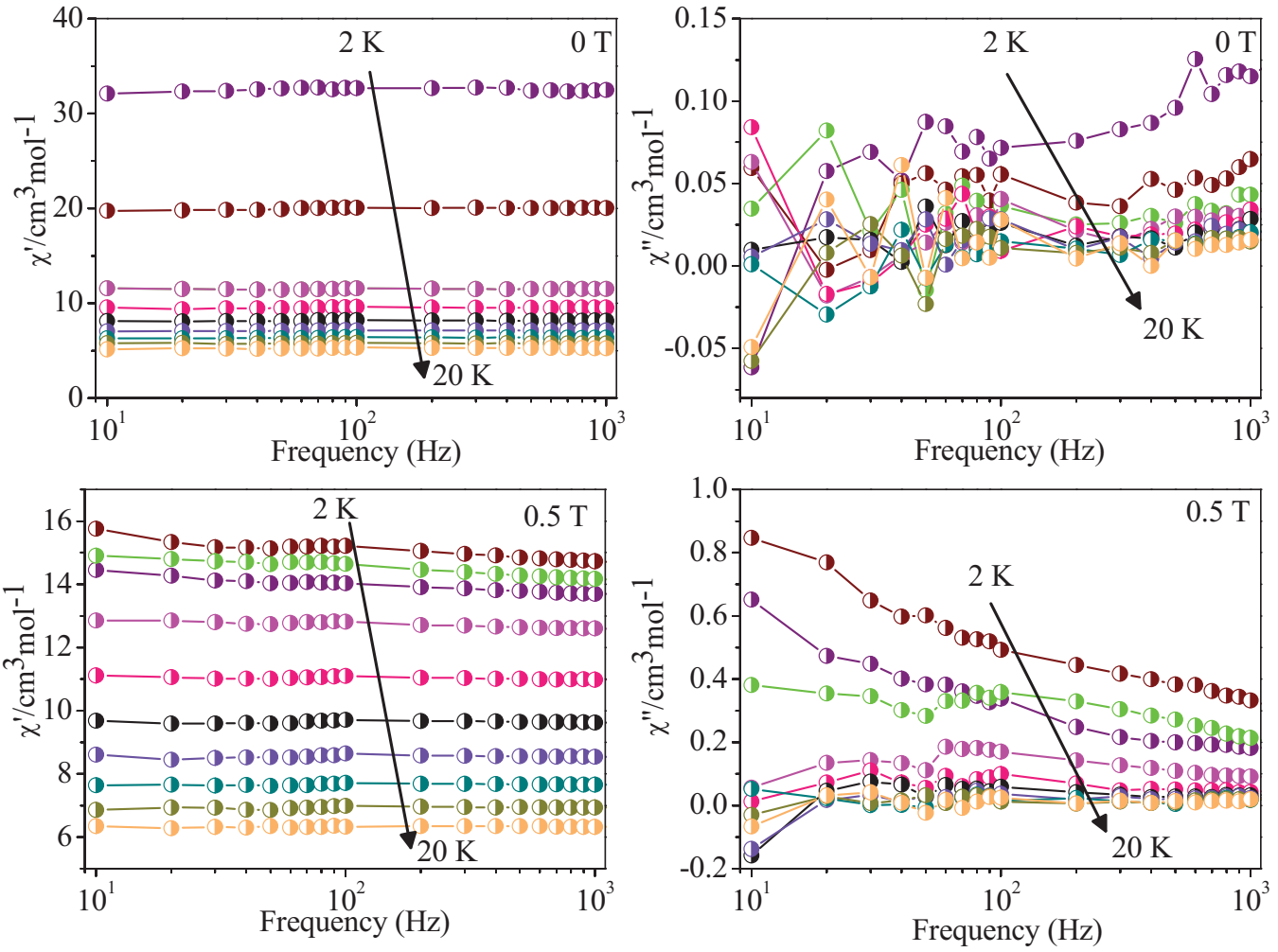

Figure S11: Frequency-dependent in-phase and out-of phase components of ac susceptibility of compound **2** under zero dc field (top) and 0.5 T field (bottom).

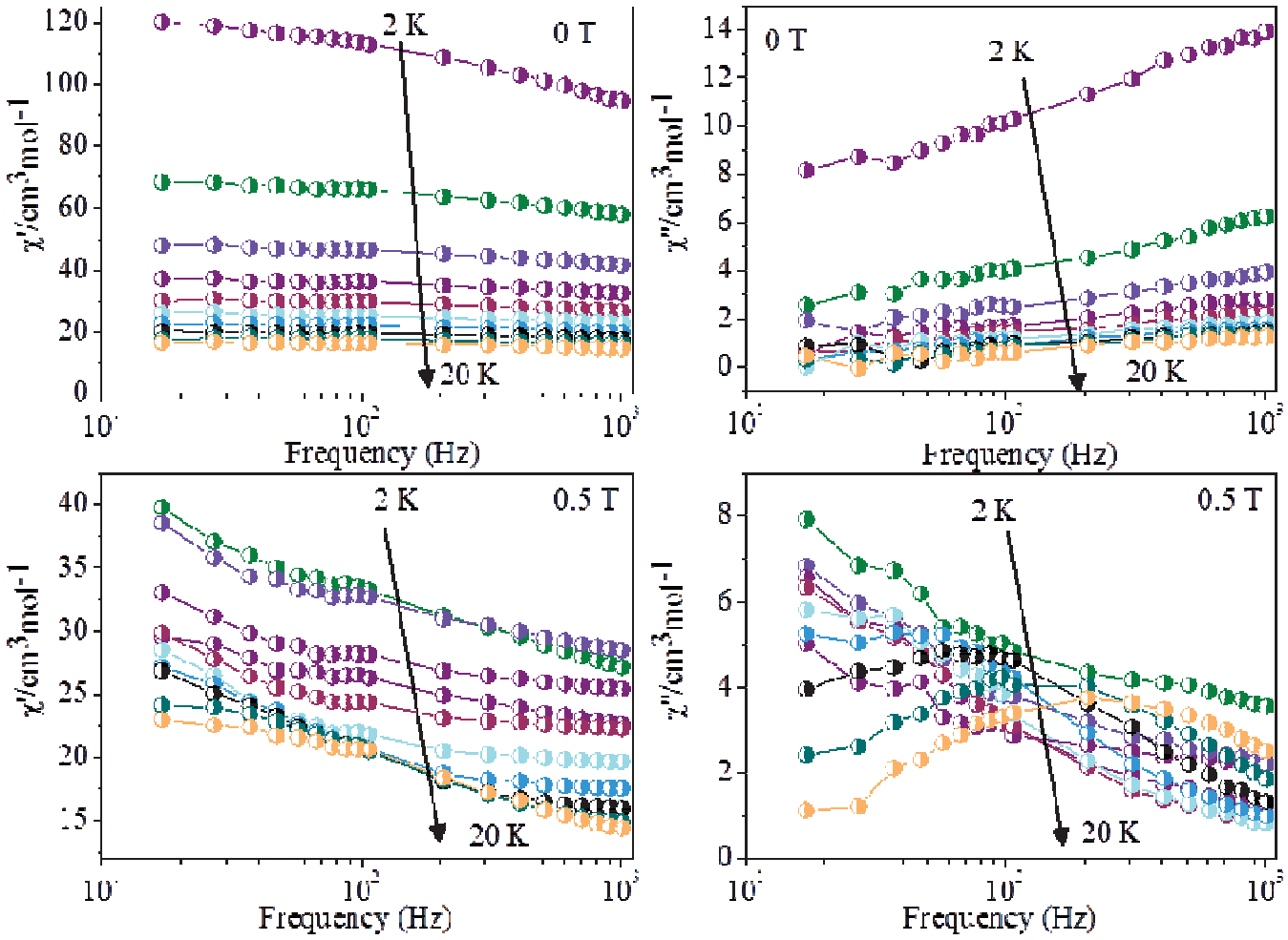

Figure S12: Frequency-dependent in-phase and out-of phase components of ac susceptibility of compound **3** under zero dc field (top) and 0.5 T field (bottom).

Table S1. Crystal data and structure refinement parameters for complexes **1-4**.

	Complex 1	**Complex 2**	**Complex 3**	**Complex 4**
empirical formula	$C_{78}H_{88}Cl_4N_{28}O_{18}Dy_8$	$C_{76}H_{80}Cl_4N_{28}O_{16}Tb_8$	$C_{108}H_{114}N_{34}O_{28}Dy_8$	$C_{120}H_{126}N_{38}O_{30}Nd_6$
formula weight	3147.56	3054.84	3636.33	3446.03
crystal system	Monoclinic	Monoclinic	Triclinic	Hexagonal
space group	*C2/c*	*C2/c*	*P-1*	$P3_22_1$
a/Å	24.237(7)	24.275(1)	14.4489(7)	16.7861(4)
b/Å	19.982(6)	20.1097(10)	16.4770(9)	16.7861(4)
c/Å	24.195(7)	24.122(1)	18.7596(10)	47.371(2)
α/°	90	90	110.305(2)	90
β/°	101.124(7)	101.093(2)	110.042(2)	90
γ/°	90	90	94.732(2)	120
$V/Å^3$	11497(6)	11555.7(10)	3830.8(3)	11559.7(7)
reflections collected	60148	80093	52086	166758
unique reflection	11904	13954	16942	21876
observed reflections[I>2σ(I)]	10348	9295	8841	9864
R1	0.0712	0.0503	0.0625	0.0856
wR2	0.2037	0.1491	0.1516	0.1965
CCDC no.	1027809	1027811	1027808	1027810

Table S2. Selected bond lengths and angles of complexes 1-4

Complex 1

Dy_1-O_{1S}	2.308(6)	Dy_2-O_1	2.381(6)	Dy_3-N_{3A}	2.441(8)	Dy_4-Dy_3	3.7640(11)
Dy_1-O_{2WS}	2.352(6)	Dy_2-N_{2A}	2.413(8)	Dy3-O_{1A}	2.469(6)	Dy_4-Dy_2	3.8205(11)
Dy_1-O_{1A}	2.353(6)	Dy_2-N_5	2.503(8)	Dy_3-O_1	2.482(6)	Dy_1-O_{2WS}-Dy_3	109.6(2)
Dy_1-N_2	2.470(8)	Dy_2-N_6	2.556(8)	Dy3-Dy_4	3.7323(11)	Dy_1-O_{2WS}-Dy_4	107.0(2)
Dy_1-N_{5A}	2.513(7)	Dy_2-Cl_2	2.674(2)	Dy_3-Dy_4	3.7640(11)	Dy_2-O_{2SA}-Dy4	110.5(2)
Dy_1-N_{6A}	2.591(8)	Dy_2-N_{1A}	2.773(8)	Dy_4-O_{2S}	2.338(6)	Dy_3-O_{2S}-Dy_4	108.8(2)
Dy_1-Cl_1	2.703(2)	Dy_2-Dy_4	3.8205(10)	Dy_4-O_{1SA}	2.339(6)	Dy_1-O_{1S}-Dy_4	110.8(2)
Dy_1-N_1	2.775(8)	Dy_2-Dy_3	3.8612(9)	Dy_4-O_{2SA}	2.352(6)	Dy_2-O_{1WS}-Dy_3	108.9(2)
Dy_1.D_{y4}	3.8476(9)	Dy_3-O_{2S}	2.253(6)	Dy_4-O_{1S}	2.367(6)	Dy_2-O_{1WS}-Dy_4	106.2(2)
Dy_1-Dy_3	3.8792(11)	Dy_3-O_{1SA}	2.275(6)	Dy_4-O_{1WS}	2.426(6)	Dy_3-O_{1WS}-Dy_4	102.7(2)
Dy_1-O_{2SA}	2.299(6)	Dy_3-O_{1WS}	2.394(6)	Dy_4-O_{2WS}	2.435(6)	Dy_3-O_{2WS}-Dy_4	101.2(2)
Dy_2-O_{1WS}	2.352(6)	Dy_3-O_{2WS}	2.395(6)	Dy_4-N_{1S}	2.533(7)	Dy_3-O_{1SA}-Dy_4	109.3(2)
		Dy3-N3	2.440(7)	Dy_4-N_{1SA}	2.548(7)	Dy_2-O_1-Dy_3	105.1(2)

Complex 2.

Tb_1-O_{1SA}	2.251(5)	Tb_2-O_{1A}	2.352(6)	Tb_3-N_{1S}	2.531(8)	Tb_1-O_{2S}-Tb_3	109.8(2)
Tb_1-O_{2S}	2.267(6)	Tb_2-O_{1W}	2.359(5)	Tb_3-N_{1SA}	2.536(7)	Tb_1-O_{1W}-Tb_3	101.6(2)
Tb_1-O_{2W}	2.372(5)	Tb_2-N_2	2.465(7)	Tb_3-Tb_1	3.7348(6)	Tb_1-O_{1SA}-Tb_3	109.5(2)
Tb_1-O_{1W}	2.398(6)	Tb_2-N_{5A}	2.515(7)	Tb_3-Tb_4	3.8251(5)	Tb_2-O_{2SA}-Tb_3	111.1(2)
Tb_1-N_{3A}	2.411(7)	Tb_2-N_{6A}	2.588(8)	Tb_3-Tb_2	3.8433(5)	Tb_1-O_{2W}-Tb_3	103.2(2)
Tb_1-N_3	2.445(7)	Tb_2-Cl_1	2.685(3)	Tb_4-O_{1S}	2.292(6)	Tb_2-O_{1W}-Tb_1	108.8(2)
Tb_1-O_{1A}	2.467(5)	Tb_2-N_1	2.777(7)	Tb_4-O_{2W}	2.336(6)	Tb_2-O_{1W}-Tb_3	107.1(2)
Tb_1-O_1	2.501(5)	Tb_2-Tb_3	3.8433(5)	Tb_4-O_1	2.361(6)	Tb_2-O_{1A}-Tb_1	106.8(2)
Tb_1-Tb_3	3.7348(6)	Tb_3-O_{1SA}	2.321(6)	Tb_4-N_{2A}	2.418(8)	Tb_4-O_1-Tb_1	105.0(2)
Tb_1-Tb_3	3.7585(6)	Tb_3-O_{2S}	2.328(6)	Tb_4-N_5	2.508(7)	Tb_4-O_{1S}-Tb_3	110.6(2)
Tb_1-Tb_4	3.8583(6)	Tb_3-O_{1S}	2.360(6)	Tb_4-N_6	2.568(8)	Tb_4-O_{2W}-Tb_1	110.1(2)
Tb_1-Tb_2	3.8688(6)	Tb_3-O_{2SA}	2.372(6)	Tb_4-Cl_2	2.645(3)	Tb_4-O_{2W}-Tb_3	106.9(2)
Tb_2-O_{2SA}	2.288(6)	Tb_3-O_{1W}	2.419(5)	Tb_4-N_1	2.769(8)		
		Tb_3-O_{2W}	2.425(5)				

Complex 3

Dy_1-O_2	2.299(6)	Dy_2-O_{2S}	2.343(7)	Dy_3O_2	2.396(6)	Dy_4-N_{1B}	2.690(9)
Dy_1-O_1	2.356(6)	Dy_2-O_1	2.357(6)	Dy_3-O_{3S}	2.448(9)	Dy_1-O_{6S}-Dy_1	111.4(2)
Dy_1-$O_{3S'}$	2.376(11)	Dy_2-O_{1S}	2.360(6)	Dy_3-O_{1S}	2.470(6)	Dy_1-O_{6S}-Dy_3	106.7(2)
Dy_1-O_{1S}	2.392(7)	Dy_2-O_{1B}	2.361(6)	Dy_3-N_{5B}	2.501(8)	Dy_1.O_1-Dy_2	114.0(3)
Dy_1-O_{6S}	2.393(6)	Dy_2-N_3	2.386(8)	Dy_3-Dy_1	3.8424(6)	Dy_1-O_{1S}-Dy_3	99.9(2)
Dy_1-O_{6S}	2.406(6)	Dy_2-N_{3B}	2.404(7)	Dy_4-O_{2A}	2.221(8)	Dy_1-O_2-Dy_3	109.8(3)
Dy_1-O_{4S}	2.464(7)	Dy_2-N_{3A}	2.454(8)	Dy_4-O_{1D}	2.421(8)	Dy_2-O_{1S}-Dy_1	112.6(3)
Dy_1-N_5	2.519(8)	Dy_2-O_{1A}	2.491(6)	Dy_4-N_{2B}	2.439(9)	Dy_2-O_{1S}-Dy_3	108.8(2)
Dy_1-Dy_3	3.7217(7)	Dy_2-Dy_3	3.9271(7)	Dy_4-O_{1A}	2.445(6)	Dy_3-O_{6S}-Dy_1	101.6(2)
Dy_1-Dy_3	3.8424(6)	Dy_3-O_{2B}	2.265(7)	Dy_4-N_2	2.462(8)	Dy_3-O_{1B}-Dy_2	113.2(2)
Dy_1-Dy_2	3.9532(7)	Dy_3-O_{7S}	2.311(7)	Dy_4-O_{1DA}	2.467(10)	Dy_4-O_{1A}-Dy_2	123.2(3)
Dy_1-Dy_1	3.9657(10)	Dy_3-O_{1B}	2.343(6)	Dy_4-N_{5A}	2.496(10)		
		Dy_3-O_{6S}	2.395(6)	Dy_4-N_1	2.619(9)		

Complex 4

Nd_1-O_{1D}	2.420(19)	Nd_2-O_{1B}-Nd_3	110.1(3)
Nd_1-O_{1A}	2.424(8)	Nd_3-O_{1W}-Nd_1	96.9(3)
Nd_1-O_{1A}	2.424(8)	Nd_4-O_1-Nd_1	121.6(3)
Nd_1-O_{2A}	2.455(9)		
Nd_1-O_{2A}	2.455(9)		
Nd_1-O_{1W}	2.528(10)		
Nd_1-O_{1W}	2.528(10)		
Nd_1-N_{5A}	2.592(12)		
Nd_1-N_{5A}	2.592(12)		
Nd_1-Nd_3	3.7390(9)		
Nd_2-O_{2B}	2.353(10)		
Nd_2-O_{2B}	2.353(10)		
Nd_2-O_{1W}	2.458(9)		
Nd_2-O_{1W}	2.458(9)		
Nd_2-O_{1B}	2.513(8)		
Nd_2-O_{1B}	2.513(8)		
Nd_2-N_{5B}	2.661(12)		
Nd_2-N_{5B}	2.661(12)		
Nd_3-O_{1W}	2.469(7)		
Nd_3-O_{2A}	2.484(10)		
Nd_3-O_{1A}	2.491(9)		
Nd_3-O_{1WS}	2.505(10)		
Nd_3-N_{3A}	2.534(11)		
Nd_3-N_{3B}	2.549(12)		
Nd_3-O_{1B}	2.576(9)		
Nd_3-O_1	2.609(8)		
Nd_3-N_3	2.615(11)		
Nd_4-O_2	2.297(9)		
Nd_4-O_{4N}	2.405(12)		
Nd_4-O_1	2.513(8)		
Nd_4-N_{2A}	2.515(11)		
Nd_4-O_{1SS}	2.54(2)		
Nd_4-N_{2B}	2.543(13)		
Nd_4-N_5	2.598(12)		
Nd_4-N_{1A}	2.71(1)		
Nd_4-N_{1B}	2.760(13)		
Nd_1-O_{2A}-Nd_3	130.8(8)		
Nd_1-O_{1A}-Nd_3	99.1(3)		
Nd_2-O_{1W}-Nd_1	110.1(3)		
Nd_2-O_{1W}-Nd_3	115.7(3)		

References:

S1. (a) Alexandropoulos, D. I; Mukherjee, S; Papatriantafyllopoulou, C; Raptopoulou, C. P; Psycharis, V; Bekiari, V; Christou, G; Stamatatos, T. C. *Inorg. Chem.***2011**, *50*, 11276−11278.(b) Canaj, A. B; Tzimopoulos, D. I; Philippidis, A; Kostakis, G. E; Milios, C. J. *Inorg. Chem*. **2012**, *51*, 7451-7453.